Separation Science and Technology
Publication details, including instructions for authors and subscription information:
http://www.informaworld.com/smpp/title~content=t713708471

Design and Testing of an Emulsion Liquid Membrane Pilot Plant

G. R. M. Breembroek[a]; G. J. Witkamp[a]; G. M. Van Rosmalen[a]
[a] LABORATORY FOR PROCESS EQUIPMENT, DELFT UNIVESITY OF TECHNOLOGY, CA DELFT, THE NETHERLANDS

Online publication date: 08 July 2000

To cite this Article Breembroek, G. R. M. , Witkamp, G. J. and Van Rosmalen, G. M.(2000) 'Design and Testing of an Emulsion Liquid Membrane Pilot Plant', Separation Science and Technology, 35: 10, 1539 — 1571
To link to this Article: DOI: 10.1081/SS-100100240
URL: http://dx.doi.org/10.1081/SS-100100240

SEPARATION SCIENCE AND TECHNOLOGY, **35**(10), pp. 1539–1571, 2000

Design and Testing of an Emulsion Liquid Membrane Pilot Plant

G. R. M. BREEMBROEK, G. J. WITKAMP,* and
G. M. VAN ROSMALEN
LABORATORY FOR PROCESS EQUIPMENT
DELFT UNIVESITY OF TECHNOLOGY
LEEGHWATERSTRAAT 44, 2628 CA DELFT, THE NETHERLANDS

ABSTRACT

An emulsion liquid membrane (ELM) extraction rotating disc contactor (RDC) column with auxiliary equipment has been designed and tested. An ELM spray column was designed as well. ELM is a suitable technique for the removal of heavy metal ions from waste or process streams. However, no design rules are available yet. This paper proposes and verifies a design procedure based on solvent extraction methods. The equipment was designed to reduce the 100 ppm cadmium concentration in a 90 L/h feed stream to 5% of its initial value, and to achieve a concentration factor of at least 12.5 in the strip phase. Trilaurylamine (1%) in kerosene was used as the extractant solution. The RDC column diameter was 70 mm and its designed height was 2.2 m. The spray column had a diameter of 50 mm and a designed height of 4.2 m. Both columns were constructed from five separate parts of 1 m height each to obtain the necessary flexibility. Experiments showed a reduction of the cadmium content down to 1% of the initial value and a concentration factor of 14 with the RDC. The efficiency of the spray column experiment was 50%. The rotor speed and the hold up in the RDC had to be kept lower (0.75 and 0.55 times, respectively) than the design values to avoid entrainment of the smallest drops with the feed phase. The validity of the models used in the design was assessed by inserting the actual experimental conditions in the design equations. This resulted in a good coincidence of the actual and calculated characteristic drop velocity, a good coincidence of most mass transfer coefficients, and a reasonable estimation of the number of equilibrium stages. The auxiliary equipment, comprising among others an electrostatic emulsion splitter, operated as designed at optimal conditions. The splitter proved to be critical at smaller emulsion droplet sizes. It can be concluded that design methods for a solvent extraction column are suitable for ELM.

* To whom correspondence should be addressed.

INTRODUCTION

Liquid membranes can be used to extract trace amounts of heavy metal ions from process or wastewater streams. The liquid membrane is a thin layer of an organic phase which separates two aqueous phases, the feed phase and the strip phase. An extractant is dissolved in the organic phase. It acts as a shuttle, extracting the metal ion from the feed phase and releasing it again at the other side of the membrane (see Fig. 1).

An advantage of the liquid membrane process is that a high concentration factor can be reached in a single process step. The combination of extraction and stripping also promotes a relatively high transport rate because, in general, the system is far from equilibrium. An additional advantage is the small amount of organic phase needed (1, 2). A recent overview on liquid membranes by Sastre et al. (3) addresses many aspects of this promising technique.

There are two basic configurations for the liquid membrane process. In the first, the membrane is obtained by absorbing the organic phase into a solid support, yielding a so-called supported liquid membrane or SLM system. In the second type the liquid membrane is the oil phase of a water-in-oil emulsion that is dispersed as emulsion drops into the feed phase. This is called an emulsion liquid membrane or ELM system (see Fig. 2). In this study, ELM extraction is applied for the purification of a cadmium-contaminated stream as an example.

The ELM process involves the preparation of an emulsion, the dispersion and contacting of the emulsion with the contaminated feed phase, and the splitting of the emulsion in the loaded strip phase and the organic phase. The latter is reused to prepare a fresh emulsion, as illustrated in Fig. 3.

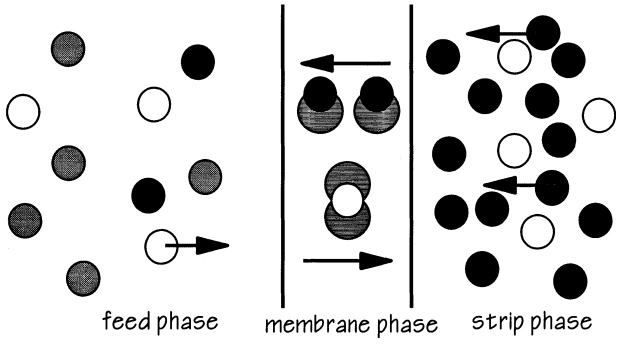

FIG. 1 Liquid membrane extraction. The concentration gradient of ● over the membrane causes the concentration of ○ in the strip phase.

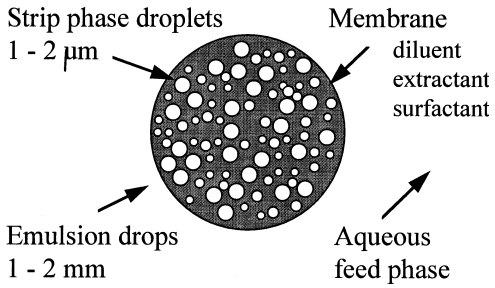

FIG. 2 Schematic representation of an emulsion liquid membrane.

In order to apply such a process, design rules for ELM columns are needed, but they are not available yet. The aim of this work is to develop a design procedure for an ELM column. It is based on the rules for solvent extraction processes. The design was validated by experiments. The experimentally adaptable parameters, such as the feed flow rate and the rotor speed, were in particular varied to optimize the extraction efficiency.

DESIGN

Requirements for the Capacity and Extraction Efficiency of the Column

The process must treat a throughput φ_{feed} of 90 L/h ($= 2.5 \times 10^{-5}$ m^3/s) containing 100 ppm (mg/kg) of cadmium, extract 95% of this amount, and achieve a concentration factor of 12.5. The splitter (see Fig. 4) should be able to split 90% of the strip phase present in the disperse phase flow.

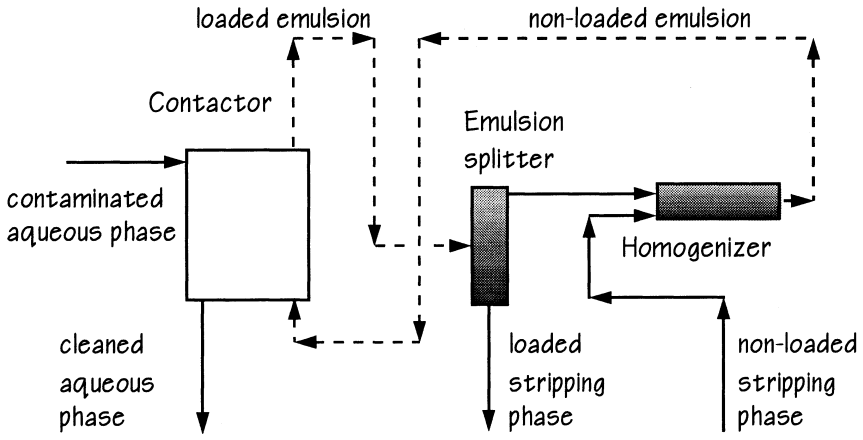

FIG. 3 Schematic flow sheet emulsion liquid membrane extraction process.

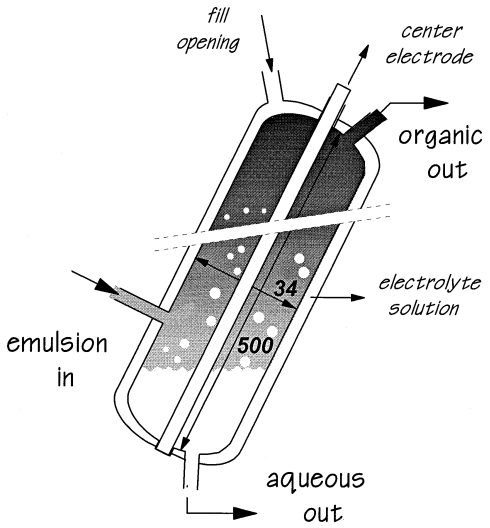

FIG. 4 Electrostatic emulsion splitter: organic phase represented by black; aqueous phase clear.

The Chemical System

Cadmium is extracted into the organic (membrane) phase as a cadmium chloride complex with tri-*n*-dodecyl amine (= trilaurylamine or TLA, with the trade name Alamine 304), 90% pure, dissolved in a half-aliphatic, half-naphthenic kerosene. The extraction of cadmium as a chloride complex will be applicable in the phosphoric acid industry, where cadmium enters the process via the ore. The extractant Alamine 304 was chosen for its selectivity for cadmium over calcium at a low pH in the presence of 0.5 M Cl^- (0.1 M HCl, 0.4 M NaCl).

The membrane phase also contained the surfactant ECA 4360J to stabilize the emulsion of the strip and the membrane phase. Its active component content is 50%. More information on its chemical structure can be found in Ref. 4. This surfactant is preferred instead of the often used Span 80 (sorbitol fatty acid ester) because its molecules do not contain oxygen. The absence of oxygen reduces the transport of water over the liquid membrane and thus the swelling and eventual leakage of strip phase from the primary emulsion (5). A drawback is that this surfactant diminishes the reaction rate at the interfaces more than does Span 80 (6).

The feed phase contains 0.5 M Cl^- to ensure the formation of cadmium chloride complexes. The strip phase contains nitrate which is exchanged for the cadmium chloride complexes and thus promotes stripping. All transport reactions are shown in Fig. 5. More information on extractions with TLA can be found in Refs. 7–10. The reaction rates are relatively high for this kind of extraction (7).

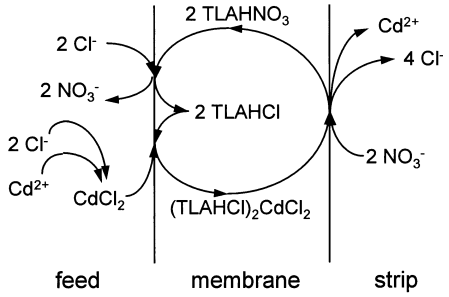

FIG. 5 Chemistry of the model extraction.

Selection of Equipment

For the ELM process, settling vessels such as are used in mixer-settler extraction equipment were not chosen. Settling is a time-consuming process that requires prolonged emulsion stability. Also, for stability reasons, a low intensity of coalescence and redispersion of the emulsion drops should be pursued. An extraction column was therefore chosen as the contactor equipment because the total residence time is equal to the contact time in this equipment. The use of mixer-settlers is reported in Refs. 3 and 11.

The RDC contactor, shown schematically in Fig. 6, was selected as the column type. The rotor discs are flat, thus effecting stirring with little breakage

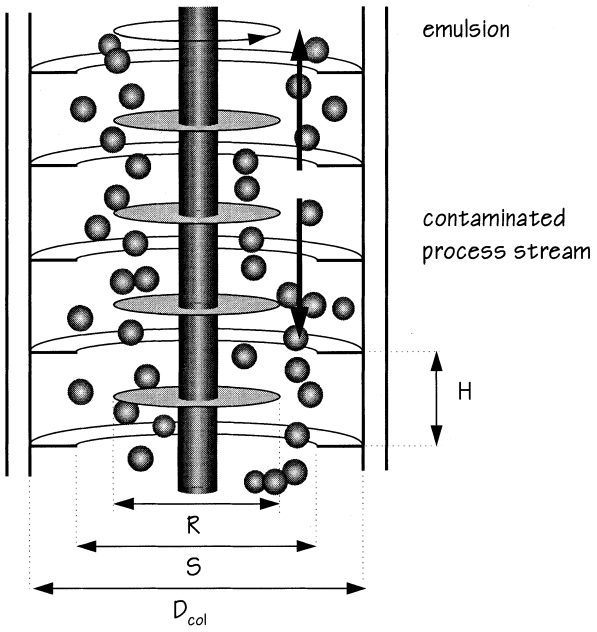

FIG. 6 Rotating disc contactor with its characteristic dimensions.

of the drops. Additionally, a spray column was designed for comparison. A spray column can be combined with the same equipment for the preparation and breakage of the emulsion, and it is easy to construct. An empty pipe with a nozzle as the emulsion inlet, a feed inlet, and feed and emulsion outlets are all that is needed.

Besides the RDC or spray contactor, equipment for the preparation and breakage of the emulsion should be provided. The preparation of the emulsion can be achieved in various ways, e.g., with an Ultra-Turrax stirrer, with a high pressure homogenizer, or by applying ultrasonic waves (12). The resulting emulsion should be stable enough to remain intact during the residence time in the contactor, but should not be too stable to prevent splitting afterwards. A hydroshear emulsifier, which operates at lower pressures than a high-pressure homogenizer, was chosen. It is relatively cheap and produces an emulsion of strip droplets in the 1 to 10 μm size range, suitable for the ELM process.

For breakage of the emulsion after contact with the feed, a method is preferred that does not change the organic phase composition. This can be achieved by heating or by exposing the emulsion to an electric field of a high voltage and a high frequency. Under the influence of this field, water droplets form chains (13), and this greatly stimulates rapid coalescence. This method was selected because the required energy input is lower than for heating. The method was successful in small-scale laboratory experiments.

Choice of Design Method and Definition of Design Parameters

Three recipes for the design of an RDC contactor for solvent extraction were found in Refs. 14–16. They often use the same equations. Zuiderweg's transparent stepwise description of the design path was followed as a guideline.

The spray column was designed using two methods. The first was the same as for the RDC, but without internals, and the second was the procedure described by Laddha and Degaleesan (14). For this last procedure, only the outcome (the required column height) will be presented.

The calculation of the dimensions of the RDC, and of the spray column according to the first method, is split into two parts:

1. Calculation of the velocities of both phases, and the dimensions of the column cross section.
2. Calculation of the column height.

Before the calculations are treated in more detail, some parameters will be defined. The extraction efficiency (Eff.) and the concentration factor in the

MARCEL DEKKER, INC.
270 Madison Avenue, New York, New York 10016

strip phase m_{real} are given by

$$\text{Eff.} = 1 - \frac{[Cd]_{\text{feed,out}}}{[Cd]_{\text{feed,in}}} \tag{1}$$

$$m_{\text{real}} = [Cd]_{\text{strip,out}}/[Cd]_{\text{feed,in}} \tag{2}$$

where the subscript "feed" designates the feed phase, "in" the inlet, "strip" the strip phase, and "out" the outlet. The hold-up h is defined as

$$h = V_{\text{disp}}/V_{\text{column}} \tag{3}$$

where V is the volume, the subscript "disp" designates the disperse phase and "column" the column, exclusive of the settling zones.

The extraction factor E is the basis for the calculation of the number of stages. In analogy with solvent extraction processes, it is defined as

$$E = \frac{\varphi_{\text{disp}} m_{\text{feed,disp}}}{\varphi_{\text{feed}}} \tag{4}$$

The variable $m_{\text{feed,disp}}$ represents the distribution coefficient of cadmium over the feed and disperse phase. As the disperse phase is a two-phase system in ELM, the value of $m_{\text{feed,disp}}$ includes two distribution coefficients, the organic/feed distribution coefficient m_{feed} and the strip/organic distribution coefficient m_{strip}. These coefficients refer to an equilibrium situation and are given by

$$m_{\text{f}} \equiv [Cd]_{\text{org}}/[Cd]_{\text{feed}}, \qquad m_{\text{s}} \equiv [Cd]_{\text{strip}}/[Cd]_{\text{org}} \tag{5}$$

All concentrations in Eq. (5) are total cadmium concentrations at equilibrium. The coefficients m_{feed} and m_{strip} can be determined by, e.g., shake tests. Together with the phase ratio $\alpha_{\text{strip,org}}$, the feed/disperse distribution coefficient $m_{\text{feed,disp}}$ can be calculated, assuming that all metal ions end up in the strip phase. This is reasonable because $m_{\text{strip}} = 80$ (see the Experimental section).

$$m_{\text{feed,strip}} = m_{\text{feed}} m_{\text{strip}}, \qquad m_{\text{feed,disp}} = m_{\text{feed,strip}} \frac{\alpha_{\text{strip,org}}}{1 + \alpha_{\text{strip,org}}} \tag{6}$$

ELM Mass Transfer, Residence Time Distribution, and Emulsion Stability

Phenomena (a) and (b) that occur during the ELM extraction process may behave dissimilar to the SX (solvent extraction) process. Phenomena (c) and

(d) only occur in ELM processes:

(a) Permeation of metal (complex) (ions) into the emulsion drops.
(b) Residence time distribution of the disperse phase in the extractor, which may affect ELM differently than SX when (a) is different.
(c) Osmotic swelling of the strip phase.
(d) Leakage of strip phase from the emulsion.

Especially for the assessment of the influence of (a) and (b), it is important to realize that the extent of internal mixing in drops in a contactor varies (17) depending on the hydrodynamics of the disperse and continuous flows. Three drop flow regimes can be distinguished: the rigid, the circulating, and the oscillating. The internal mixing increases in this sequence.

ad a. The three most important models for the calculation of the permeation of the metal ions into emulsion drops are:

(i) The hollow sphere model, which regards the emulsion drop as a bulb of strip phase inside a shell of membrane phase (18). This shell forms the mass transfer barrier.
(ii) The advancing front model (19), which is characterized by a gradual shift of the reaction front toward the center of the drop.
(iii) The reverse reaction model, which is an extension of the advancing front model (20). Recently, a modified diffusion model was presented (21, 22).

Wang and Bunge showed that (iii) should be used when competition between permeating species occurs (23). This does not lead to improvements for the current system. A characteristic of (ii) and (iii) is that the apparent mass transfer coefficient decreases with time because the diffusion path length increases. Furthermore, the drops are regarded as rigid, i.e., no internal circulation exists.

Chan and Lee (24) presented a review of these emulsion liquid membrane permeation models and concluded that the hollow sphere model could be used satisfactorily for the description of liquid membrane processes despite its simplicity. Based on their findings, this model was selected here to describe the permeation into the emulsion. A second reason is that the condition of rigid drops, which allows the application of the other two models, may not be met for the drops in the column.

The choice of the hollow sphere model implies that the permeation process can be described with one resultant mass transfer coefficient just like in solvent extraction. The design procedure thus needs no adaption in this sense.

ad b. In the hollow sphere model the resultant mass transfer coefficient is not dependent on residence time in the column, contrary to the other ELM permeation models. A description of the axial dispersion of the disperse phase in the column with an axial dispersion coefficient is therefore allowed.

in analogy to SX. The axial dispersion coefficient was also used in Ref. 25 where an ELM process was modeled. In Refs. 26 and 27 a different approach was followed: the residence time of the individual drop sizes was modeled separately while the mass transfer was modeled with the advancing front model.

ad c. Swelling is the effect that the strip phase is diluted via water transfer from the feed phase. The driving force for this process is the osmotic pressure gradient. The osmotic pressure gradient in the current chemical system, 1.3 MPa, will certainly promote water transport. The water carrier is an extractant or surfactant molecule dissolved in the organic membrane phase. As no quantitative model for swelling is known, it could not be included in the design. For experimental purposes it is possible to adapt the ionic strength of the feed phase to the strip phase, but this was not done here.

ad d. Leakage of strip phase droplets is the result of the breakage of one disperse phase drop in two, or by insufficient stability of the primary emulsion. No quantitative model for leakage is known, so it could not be included in the design. (From the experiments it appeared that leakage was strongest on entering the column, but not zero in other parts.)

Input Parameters

The input parameters for the calculation of the column dimensions are shown in Figs. 7 and 8. The concentration factor m_{real}, the feed flow φ_{feed}, the

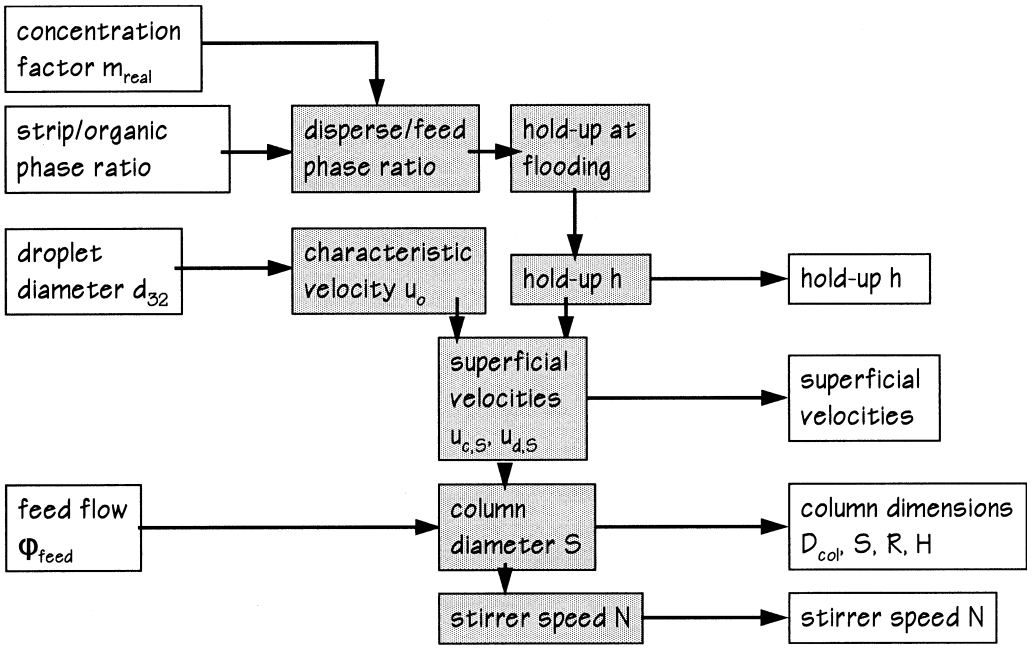

FIG. 7 Calculation of compartment dimensions and characteristics.

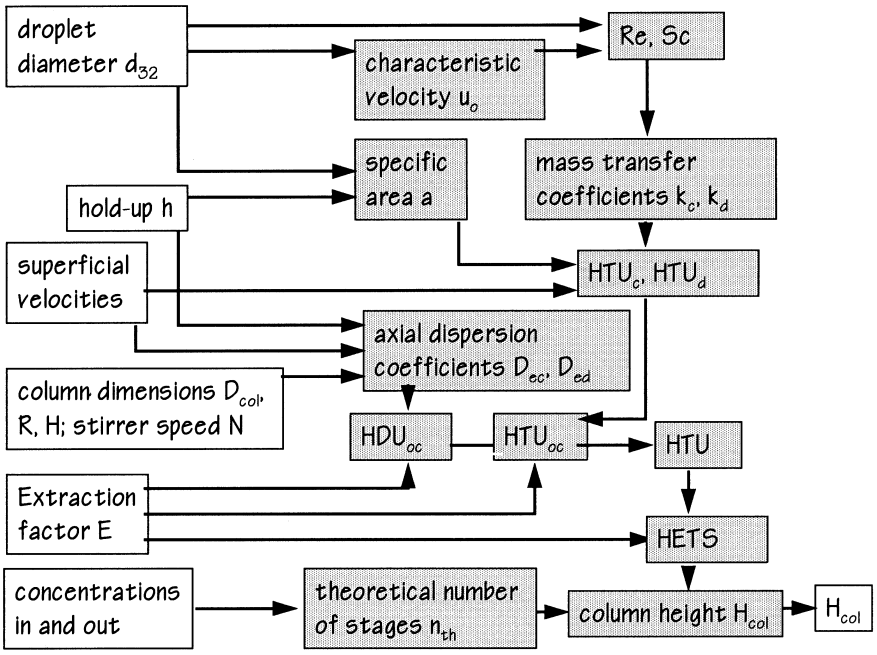

FIG. 8 Calculation of column height.

strip/organic phase volume ratio $\alpha_{strip,org}$, the Sauter diameter d_{32} of the disperse phase drops, and the extraction factor E are given in Table 1.

m_{real} and φ_{feed} are given as requirements for the design. A suitable $\alpha_{strip,org}$ was found to be 1 from preliminary experiments. From other experiments it could be concluded that a Sauter diameter of 1×10^{-3} m was the optimum size when a spraying nozzle was used. The larger the droplets the lower the surface area/volume ratio (A/V) in the column and the lower the mass transfer. At smaller drop sizes, more leakage was found as a result of the higher A/V and probably also because of shear in the nozzle. A drop size in the range of 0.1 to 2 mm is typical for ELM processes (28). The extraction factor E was calculated from Eq. (4). The value of the distribution coefficient $m_{feed,disp}$ was

TABLE 1
Input Parameters

Parameter	Value
Concentration factor m_{real} (—)	12.5
Phase ratio $\alpha_{strip,org}$ (—)	1
Drop diameter d_{32} (m)	1×10^{-3}
Feed flow φ_{feed} (m^3/s)	2.5×10^{-5}
Extraction factor E	1.6

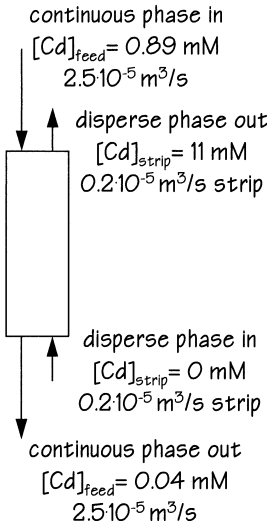

FIG. 9 Column mass balance.

10, which is a conservative value found from m_{feed} and m_{strip}, determined by preceding shake tests.

The concentrations at the inlet and outlet of the column were calculated from a mass balance. They are shown in Fig. 9, assuming that a nonloaded strip phase enters the column and that all extracted cadmium leaves the column in the strip phase. (Calculations with the experimental m_{strip} show that this assumption is reasonable.)

In addition to the mentioned input parameters, some physical properties were needed. They are given in Table 2. The disperse phase diffusion coefficient was taken to be equal to that in the organic phase. This was done because the diffusion of the cadmium–extractant complex in the organic phase is assumed to be much slower than the diffusion in the very small strip droplets, so that the rate of the diffusion through the organic phases is taken for the whole disperse phase (29). The viscosity of the disperse phase was taken as equal to that of the organic phase for the same reason. The emulsion will be non-New-

TABLE 2
Physical Properties of the System

Parameter	Feed/continuous phase	Emulsion/disperse phase
Density ρ_c, ρ_d (kg/m^3)	1000	900
Viscosity η_c, η_d (Pa·s)	1×10^{-3}	1.56×10^{-3}
Diffusion coefficient ID_c, ID_d (m^2/s)	0.72×10^{-9}	4.12×10^{-10}
Interfacial tension feed/emulsion γ (N/m)	10×10^{-3}	

tonian, but as a sensitivity analysis showed that the viscosity of the disperse phase is not a critical parameter, this approach is justified.

Calculation of Column Dimensions

A calculation scheme for the superficial velocities of continuous and disperse phase, and the dimensions of the column cross section, is given in Fig. 7, and one for the calculation of the column height in Fig. 8. All corresponding equations are given in the Appendix. Their numbers start with an A (A*x*). The characteristic column dimensions can be seen in Fig. 6. The distance between two stator rings is called a compartment.

The most important results are given in Table 3. Intermediate values can be found in Table 9 in the Appendix. The required column height for the RDC is 2.2 m, and for the spray column treated as an empty RDC a height of 4.2 m is needed. The diameter D_{col} for the RDC was 0.07 m, and for the spray column 0.05 m. The method of Laddha and Degaleesan (14) for a spray column design resulted in a required column height of 3.2 m. It was decided to construct both columns from five separate parts of 1 m each to obtain the flexibility that was necessary for the research. Those parts are referred to as sections in the rest of the paper, and consist of 20 compartments. These five sections are referred to as I to V. A settling section (VI) is located on top of the extraction sections in these designs.

Design of the Electrostatic Splitter

Various arrangements of electrodes for electrostatic splitting are put forward in the literature (5, 30–32). However, little information is given about the coalescence rate of liquid membrane emulsions. The electrostatic splitter that was selected is based on the splitter described in Ref. 5 and shown in Fig. 4.

TABLE 3
Results from the Column Compartment Calculations and Column Height

	RDC	Spray
Hold-up h (—)	0.16	0.16
Velocity continuous u_c (m/s)	0.013	0.013
Velocity disperse u_d (m/s)	0.0021	0.0021
Column diameter D_{col} (m)	0.07	0.05
Rotor diameter R (m)	0.035	—
Stator opening S (ms)	0.05	—
Compartment height H (m)	0.02	—
Rotor speed N (s^{-1})	11	—
Column height H_{col} (m)	2.2	4.2

MARCEL DEKKER, INC.
270 Madison Avenue, New York, New York 10016

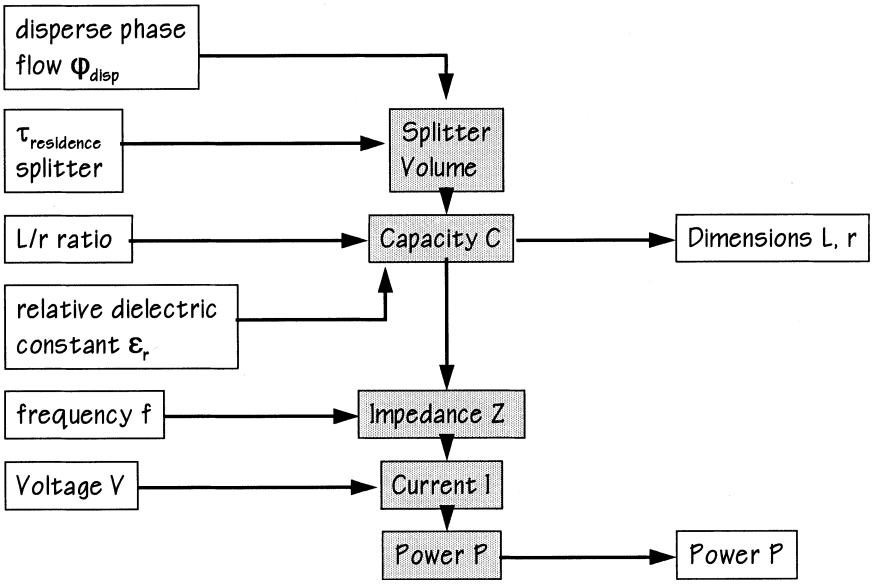

FIG. 10 Calculation of dimensions and power requirement of the electrostatic splitter.

The first electrode is formed by an electrolyte outside the splitter. The second electrode, a metal rod, is brought into direct contact with the emulsion. In this way a homogeneous field is generated.

The design path is illustrated in Fig. 10. Corresponding formulas can be found in the Appendix. The input parameter φ_{disp} can be deduced from m_{real}, as can the required extraction efficiency. The residence time needed for a 90% split and the relative dielectric constant were determined experimentally from a laboratory glass tube cooler (with an L/r ratio of approximately 30) and a high frequency generator. The diameter of the center electrode r_i was 0.003 m. The voltage and frequency to be used were determined in cooperation with Endeburg Electronics, who designed the electric circuit. The values of the input parameters are summarized in Table 4.

TABLE 4
Parameters Used for the Design of the Electrostatic Splitter

Parameter	Value
Disperse phase flow rate φ_{disp} (m^3/s)	4×10^{-6}
$\tau_{splitter}$ (s)	120
$L/r_{splitter}$ (—)	30
Center electrode r_i (m)	0.003
Relative dielectric constant, ε_r (—)	23
Frequency f (Hz)	4×10^3
Voltage V (V)	3000

The resultant apparatus had a length of 0.5 m, a radius of 0.017 m, and a power requirement of 80 W.

EXPERIMENTAL

Experimental Setup

The experimental setup, consisting of a 5 m high column and auxiliary equipment, is shown schematically in Fig. 11. Either the RDC or the spray column can be connected.

Both columns were constructed from Perspex to enable a good view of the emulsion droplets during operation of the column. They were both built from five separate extraction sections of 1 m each, which allowed the column length to be changed when needed. A sampling point was build in between two sections to allow the extraction process to be followed. On top of the extraction sections was a settling section of 0.5 m. The emulsion was fed into the RDC column through a simple tube with an internal diameter of 16 mm. The spray column was fitted with a nozzle of 3 mm internal diameter at the bottom to disperse the emulsion that was fed into the spray column.

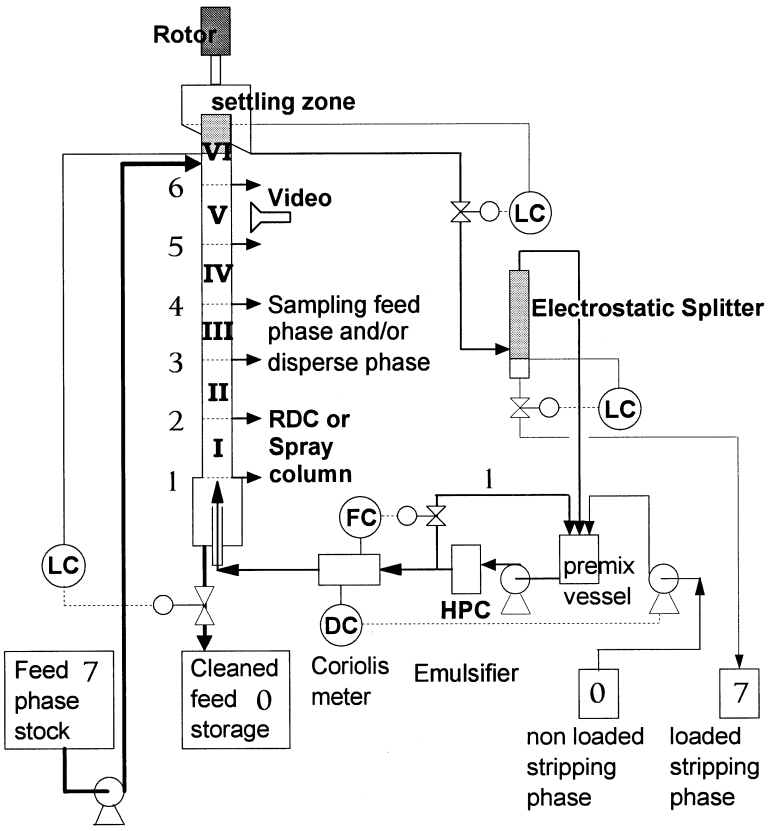

FIG. 11 ELM experimental setup.

MARCEL DEKKER, INC.
270 Madison Avenue, New York, New York 10016

A suitable emulsifying device, called a hydroshear, from APV Gaulin was used. The splitter was constructed as designed from glass, which is brittle, but which has high chemical resistance and good electrical isolating properties.

To control the flows, four process control loops were build in.

1. The level of the feed phase in the column is kept constant by a valve on the outlet.
2. The density (and thus the organic/strip phase ratio) of the emulsion flowing into the column is controlled by the influx of a nonloaded stripping phase.
3. The flow of emulsion into the column is controlled with a valve.
4. The level of loaded strip phase in the electrostatic splitter is kept constant with a valve.

Analysis

The Sauter mean diameter d_{32} was determined with a CCD camera for each section. This measurement was performed in duplicate. The total hold-up in the column was determined after each experimental run by measuring the levels in the column after arresting all streams.

The cadmium concentrations in feed and strip phases were determined by sampling and subsequent analysis with ICP-AES. The density of the emulsion and the concentration of a tracer in the strip phase were also checked to determine swelling and leakage. All these determinations were performed in triplicate.

Overview of the Experiments

An overview of the experiments with the RDC is presented in Table 5. The standard composition of the feed phase was 1 mM cadmium, 0.1 M HCl, and 0.4 M NaCl. The membrane phase was predominantly kerosene (Shellsol D70) with the extractant Alamine 304 (Henkel), with trilaurylamine (TLA) as the main constituent and surfactant (ECA 4360J). Their concentrations in the kerosene were varied as mentioned in the last two columns in Table 5. The stripping phase consisted of 1 M HNO_3 with 10 mM KNO_3 as a swelling tracer. The osmotic pressure difference between feed and strip was 1.25 MPa. The inorganic chemicals were chemically pure.

Experiments were combined in one group when they were hydrodynamically (nearly) identical but chemically different. This was justified by the results.

Some experimental conditions had to be adapted to avoid leakage of the strip phase or the build-up of small drops. The strip/organic volume phase ratio was generally 0.67 instead of 1 (as assumed in the design) to make a more stable emulsion. In the experiment with a higher surfactant concentration

TABLE 5
Experimental Conditions and Measured Hold-Up[a]

Exp.	Rotor N (s^{-1})	Feed phase φ_{feed} (m^3/s)	Disperse phase φ_{disp} (m^3/s)	ρ (kg/m^3)	Hold-up h (−)	τ_{column} (s)	Membrane phase ECA (wt%)	TLA (wt%)
A1, A2	4.3	31×10^{-6}	3.3×10^{-6}	900	0.084	510	0.5	0.5, 1.0
A3, F1								1.5, 1.0
R1	4.3	17×10^{-6}	3.3×10^{-6}	870	0.040	250	0.5	1.0
R2	5.5	17×10^{-6}	3.3×10^{-6}	870	0.050	310	0.5	1.0
R3, E1, E2,[b] N1[c]	7.6	17×10^{-6}	3.3×10^{-6}	890	0.089	530	0.5, 0.5, 1.0, 0.5	1.0
			Spray Column					
S1	—	31×10^{-6}	6.9×10^{-6}	0.90	0.059	83	0.5	1.0

[a] Rotating disc contactor (RDC). The experimental codes refer to varied parameters: A = alamine (TLA) concentration, F = feed flow rate, R = rotor speed, E = ECA concentration, N = nitrate concentration, and P = emulsifier pressure.
[b] ECA concentration 1.0 wt%.
[c] HNO_3 strip phase 2M.

MARCEL DEKKER, INC.
270 Madison Avenue, New York, New York 10016

(E2), the splitter was not used. Its capacity proved to be critical in this case, and the finer dispersed emulsion could not be split in time for recycling. During Experiment E2 an emulsion made from fresh strip *and* organic phase was fed continuously into the column.

EXPERIMENTAL RESULTS AND DESIGN DISCUSSION

Column Performance

The maximum attained column performance was an efficiency of 98%, with a concentration factor m_{real} of 15 in the strip phase, as calculated for Experiments R3, E1, E2, and N1 from measured data (Eqs. 1 and 2). These values were better than the efficiency requirement. The values for the other experiments can be found in Table 6. The lowest efficiency was found for the spray column where only 50% of the cadmium was removed. This was due to the very low residence time of the disperse phase. Because of its poor performance, the spray column will not be further discussed.

A remark that should be made regarding the efficiencies is that the RDC used was higher than originally designed. The rotor speed was lower than designed to avoid entrainment of the smallest drops with the feed phase. Because of the resulting higher average drop size, the hold-up, the specific area, and the mass transfer coefficient were also affected.

In order to get clear insight into the factors that determine the efficiency of the column, and to verify whether the design equations used are able to predict the actual experimental findings, the most important aspects of the column design will be addressed consecutively in the following sections. The mass transfer mechanism will be discussed in detail in another paper. The low efficiencies of R1 and R2 limit their relevance for future design.

Leakage varied from around the detection limit (R1, R2) up to 25% of the initial strip phase flow. It mostly occurred in the lowest column section, where the disperse phase flow was dispersed into small drops. Swelling was low ($<10\%$).

TABLE 6
Column Efficiency, Concentration Factor, and Mass Transfer Coefficients

Exp.	φ_{feed} (m^3/s)	Stirring N (s^{-1})	Eff. %	Concentration factor	Transfer coefficient k_{oc} (m/s)	Design Eqs. (A12)–(A15) k_{oc} (m/s)
A1, A2, A3, F1	31×10^{-6}	4.28	71	16	0.8×10^{-5}	0.7×10^{-5}
R1	17×10^{-6}	4.28	85	13	3.6×10^{-5}	0.4×10^{-5}
R2	17×10^{-6}	5.52	92	14	2.1×10^{-5}	0.5×10^{-5}
R3, E1, E2, N1	17×10^{-6}	7.57	98	15	0.7×10^{-5}	0.9×10^{-5}

The value of $m_{\text{feed,disp}}$ proved to be higher in practice than had been assumed in the original design. From separate experiments it was found that m_{feed} and m_{strip} were 0.5 and 80, respectively. Using the actual phase ratio $\alpha_{\text{strip,org}}$ of 0.67 in Eqs. (5) and (6), the value $m_{\text{feed, disp}} = 16$ was obtained instead of 10 that was used in the design. This actual value was used for the calculation of the mass transfer coefficient k_{oc} and for the number of equilibrium stages in subsequent sections.

Drop Size Distribution

The Sauter diameter and the hold-up for each section had to be measured for calculation of the interfacial area of the disperse phase. For this reason the drop size distribution had to be measured. As an example of the measured drop size distributions, the results of extraction sections 1, 3, and 5 for Experiment R2 are shown in Fig. 12. The drop size distribution is very broad in the first extraction section. The small drops present there apparently coalesce in the course of their residence time since fewer small drops are present in the higher column sections and no build-up of small drops occurs. This phenomenon is observed in all experiments and is typical for column section 1 only. Therefore, further analysis concentrates on sections 2–5.

The Sauter mean diameter d_{32} is calculated from the drop size distribution:

$$d_{32} = \Sigma d_i^3 / \Sigma d_i^2 \tag{7}$$

The parameter d_{32} decreases at higher rotor speeds. Its average value over the column was 3.1, 2.5, and 1.5 mm at rotor speeds of 4.3, 5.5, and 7.6 s^{-1}, respectively, for Experiments R1, R2, and R3. The influence of the chemical composition of the disperse phase, as varied in Experiments R3, E1, E2, and

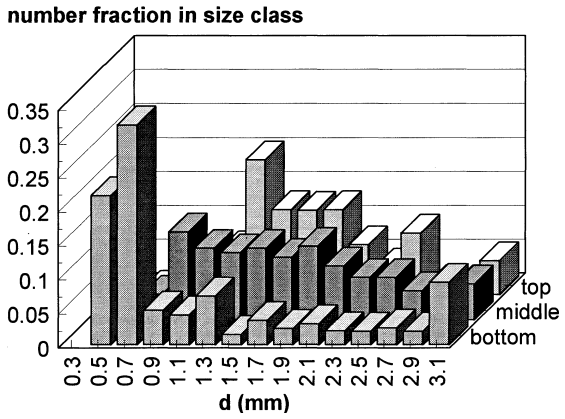

FIG. 12 Drop size distribution d_{32} during experiment R2, 5.52 s^{-1}, bottom (I), middle (III), and top (V) section.

MARCEL DEKKER, INC.
270 Madison Avenue, New York, New York 10016

N1, is minor. Furthermore, d_{32} decreases during the ascent of drops in the column.

The actual d_{32} was larger than the drop size of 1 mm, which was one of the input parameters in the original design, because of the lower rotor speed, as was explained previously. However, at higher rotor speeds so many very small droplets formed that operation is made much more difficult.

Hold-Up

The hold-up during the experiments varied from 0.04 at the lowest rotor speed up to 0.089, as can be seen from Table 5. This last value is approximately 0.55 times the value of 0.16 used in the original design. This lower value has three causes:

- d_{32} was larger than the design value, causing a shorter residence time of the disperse phase.
- It was hard to operate close to h_{flooding} since the valve that controlled φ_{disp} was not stable because of vibrations of the homogenizer. Frequent adjustments were made, but short inconsistancies could not be avoided. When operating close to h_{flooding} was attempted, those inconsistancies induced flooding.
- φ_{feed} had to be lowered to ensure good extraction. To maintain the same hold-up, φ_{strip} should have been raised. This was not done to keep the concentration factor m_{real} high enough.

The hold-up for each section was needed for the calculation of the specific area a_{spec} for each section (A16) together with d_{32}. The hold-up was calculated from the total hold-up, where the hold-up per section was regarded to be proportional to the $1/d_{32}$ in that section, as was measured by Tsouris et al. for an Oldshue–Rushton column (33). The results were confirmed by visual observations. The difference in calculated hold-up in two sections during one experiment was maximally a factor of 1.5. A maximum hold-up in the middle of the column, or an equal hold-up in each section, as found by other authors (34–36) was not observed here.

The unmentioned Experiment A2a had to be stopped because of flooding. The measured hold-up at flooding was equal to the value as calculated from Eq. (A2). Another experiment, not further described in this paper, confirmed this. This supports the use of the SX design method for the design of the column diameter D_{col}, and the related sizes, for this ELM process.

Characteristic Velocity of the Drops

The characteristic velocity u_0 of the drops corresponds to their slip velocity u_s with a correction for their presence in a swarm of drops.

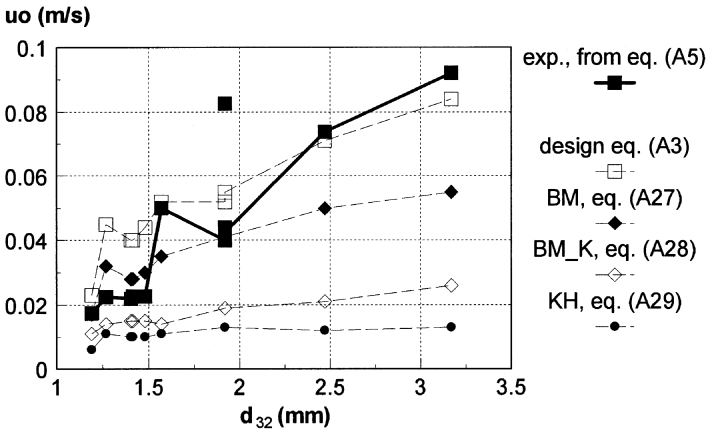

FIG. 13 Experimental values and model predictions of characteristic velocity u_0 as a function of d_{32}. Lines serve to guide the eye.

The prevailing values of u_0 are plotted against d_{32} in Fig. 13 as filled squares. They are calculated from Eq. (A5) and averaged over all sections. d_{32} is the most important variable that influences u_0 in the presented experiments. The experimental values of h, $\alpha_{disp,feed}$, and $u_{c,S}$ (the superficial velocity of the continuous phase through the Stator ring opening) were used for the calculation of u_0. The values of u_0 were sometimes higher and sometimes lower than the design value of 0.034 m/s (see Table 9 in the Appendix) because the experimental conditions differed from the original design.

In Fig. 13 values of u_0 are also plotted that were calculated by inserting the experimental conditions (e.g., $\Delta\rho$, u_c) into four correlations:

1. The design u_0 Eq. (A3).
2. The correlation of Barnea and Mizrahi (BM) (A27).
3. The correlation of Korchinsky, as a modification of those proposed by BM (BM_K) (A28).
4. The correlation of Kumar and Hartland (KH) (A29).

The correlations BM and BM_K calculate u_0 for all individual drop sizes. Again, the average over the whole column is presented. The curves in Fig. 13 are not smooth because the density difference is also a parameter in the equations and it is not the same in all experiments.

The design Eq. (A3) roughly describes the trend in the experimental results. At drop sizes beneath 2 mm, the equation of Barnea–Mizrahi produces a somewhat better fit between the experimental and modeled u_0 values than the design equation. On the whole, however, the design equation provides a good estimation for u_0.

The models BM, BM_K, and KH require experimental input data. BM_K, for instance, uses a constriction factor to be determined from the measured superficial velocities, the hold-up, and the drop-size distribution. Further investigation is necessary to find out why the fit is unsatisfactory.

MARCEL DEKKER, INC.
270 Madison Avenue, New York, New York 10016

Overall Mass Transfer Coefficient k_{oc}

The overall mass transfer coefficients k_{oc} were calculated per section from the interfacial area calculated from the measured h and from d_{32}, the measured mass transfer (mol/s), and the concentration in the feed phase. The averages of these k_{oc}'s over Sections II to V are shown in Table 6. The difference between k_{oc} values for hydrodynamically similar but chemically different experiments was very small. The lowest column section was omitted from the calculation because leakage from the strip droplets occurred there, while leakage and swelling were low in the higher column sections (37).

The measured overall mass transfer coefficients k_{oc} lie in the same range as the value of 1.9×10^{-5} m/s used in the design (see Table 7). The value of k_{oc} decreases with increasing rotor speed or increasing flow rate, and hence with decreasing drop size. This is probably due to the presence of more rigid drops at a lower drop size (17). The relation between the large drop size (Experiments R1 and R2) and the high mass transfer coefficient will be treated in more detail in another paper.

The applicability of the design equations for k_{oc} (A15) was checked. First k_d (A12) and k_c (A13) were calculated with the measured drop size d_{32} and u_0 from Eq. (A5) as input parameters. Then (A15) was used to calculate k_{oc}. The results can be compared to the measured k_{oc} in Table 6. It can be concluded that k_{oc} is underestimated by the model for Experiments R1 and R2 where the drop size was larger than in the other experiments. On the other hand, k_{oc} can be predicted well for the experimental series A1, A2, A3, F1 and R3, E1, E2, N1. These last four experiments are the most relevant ones for a future design because their efficiency was 98%.

The resistances $1/k_c$ and $1/(m_{feed,disp}k_d)$ (see A15) were compared to find the main resistance for transport. According to the design equations, the resis-

TABLE 7
Height of Transfer Units and Number of Equilibrium Stages

Exp.	Eff. (—)	Transfer coefficient k_{oc} (m/s)	E (—)	Specific area a_{spec} (m^{-1})	HTU_{oc}[a] (m)	HTU (m)	$n_{calc,HETS}$[b] (—)	n_{meas}[b] (—)
Design		1.9×10^{-5}	1.6	945	0.36	0.40	10	
A1, A2, A3, F1	71	7.7×10^{-6}	1.8	270	3.7	3.8	0.81	1.2 ± 0.2
R1	85	3.6×10^{-5}	3.2	76	1.6	1.6	1.5	0.4
R2	92	2.1×10^{-5}	3.2	122	1.7	1.7	1.4	1.6
R3, E1, E2, N1	98	7.2×10^{-6}	3.2	390	1.5	1.6	1.5	2.4 ± 0.1

[a] $HDU_{oc} < 0.03$ m for all experiments.
[b] Only the upper four column sections were regarded.

MARCEL DEKKER, INC.
270 Madison Avenue, New York, New York 10016

tance is predominantly located in the disperse phase (only 4 to 13% in the aqueous phase). k_c is thus large compared to k_{oc}. To enhance the mass transfer rate, efforts should therefore be focused on the dispersed phase.

Number of Equilibrium Stages

The values of n_{meas}, the number of equilibrium stages over the upper four column sections, were calculated from the measured concentrations at sample points 2 and 6 using Eq. (A23). They are given in the last column of Table 7 for all experimental series. The bottom column section was omitted from this calculation because of leakage of the strip phase.

The applicability of the design Eqs. (A16) to (A21) and (A24) is assessed by calculating the number of stages $n_{calc,HETS}$ from HETS (A24). First, HTU_{oc} was calculated using measured values of k_{oc}, the interfacial area a_{spec}, and u_c (Eqs. A16 and A17). Second, HDU_{oc} was calculated using Eqs. (A18)–(A20) with the actual $u_{c,Dcol}$ and $u_{d,Dcol}$. HDU_{oc} was smaller than 0.03 m, which implies that the axial dispersion, where HDU_{oc} is a measure for, was small. From HTU_{oc} and HDU_{oc}, HTU can be calculated (Eq. A21). With the extraction factor E based on $m_{feed,disp} = 16$, HETS can be found (Eq. A22). Finally, $n_{calc,HETS}$ follows from Eq. (A24), analogous to n_{th}, using the $H_{col} = 4$ m.

The values for the original design are also included in Table 7 for easy comparison with the experimental values. A column height of 4 m was also taken here.

The heights of the transfer unit (HTUs) are larger than the original design value, mostly because of the smaller specific area, a_{spec}. This area is at least a factor 2.5 smaller than the designed value due to the low hold-up and the larger drops. Consequently, the number of equilibrium stages is much lower than the original design value of 10, whether it is directly measured ($n_{meas} = 0.4–2.4$) or calculated ($n_{calc,HETS} = 0.8–1.5$). Although the HTU is larger than designed, the extraction was successful (especially series R3) because of the higher extraction factor E and the larger column height than designed.

The calculated number of stages $n_{calc,HETS}$ is approximately equal for R1, R2, and the R3 series as can be concluded from the second column from the right in Table 7, while the measured number n_{meas} is increasing in the order R1 $<$ R2 $<$ R3 series (last column). No explanation for this increase could be found.

The process becomes more effective as the approach to the design conditions is closer. A closer approach to the design conditions than in Experiments R3, E1, E2, and N1 proved difficult because of entrainment of small droplets. For future designs it is recommended that an actual drop size distribution should be determined during the design.

MARCEL DEKKER, INC.
270 Madison Avenue, New York, New York 10016

Auxiliary Equipment

The Sauter mean diameter of the strip phase droplets varied from 8 μm down to 4 μm in Experiment E2 at a higher surfactant (ECA) concentration. At a magnitude of 8 μm, the subsequent splitter operation was good.

The splitter operated at 4 kV and 3 kHz. The electric capacitance of the system was lower than expected because of losses over the water layer which was more conductive than the oil layer. The contents of the splitter were regarded as a continuum in the design, which proved to be an unacceptable simplification. During the experiments the water level was kept low to minimize the effect on splitter efficiency.

The splitter efficiency was generally around 85%, see Table 8. This was 5% lower than the design value but still sufficient. The emulsifier concentration should not be too high because this causes a low splitting rate, as seen in Experiment E2.

General Comments Related to Future Design and Operation

Based on all these results, a few recommendations for future design can be made. First, the rotor speed must be variable in order to prevent the formation of too small drops. Separate experiments to determine a good drop size are recommended. This size should be small enough to stimulate mass transfer, but entrainment should be avoided. When the rotor speed is adjusted, the efficiency of the column changes. A safety margin for the column height is therefore advised. For this column, a factor of 1.8 was needed. This is a large number because the actual d_{32} was significantly larger than in the original design. Furthermore, a pump should be installed to transfer the emulsion into the column. In this way small pressure fluctuations in the hydroshear emulsifier do not cause fluctuations in the emulsion flow φ_{disp} into the column. For the range

TABLE 8
Strip Drop Size and Splitter Efficiency

Exp.	ECA (%wt)	φ_{disp} (m^3/s)	d_{32}, strip (μm)	$\tau_{splitter}$ (s)	Split efficiency (—)
A1, A2, A3, F1	1.0	12	8	140	0.92
R1	1.0	12	8	140	0.95
R2	1.0	12	8	140	0.85
R3, E1, N1	1.0	12	8	140	0.78
E2[a]	2.0	12	4	140	—

[a] Splitter not used.

MARCEL DEKKER, INC.
270 Madison Avenue, New York, New York 10016

of operating conditions tested in this study, the design equations describe the actual operation adequately.

CONCLUSIONS

An emulsion liquid membrane RDC extraction column for the extraction of cadmium from a 90 L/h feed phase containing 100 ppm Cd was designed for an extraction efficiency of 95%, and it was operated under varying conditions. The design was based on rules for solvent extraction columns. The constructed column had a diameter of 70 mm and consisted of five separate parts with a height of 1 m each. The maximal efficiency of a group of experiments was 98%, and the corresponding concentration factor in the strip phase was 14.

The rotor speed and the hold-up had to be adjusted to 0.75 and 0.55 times their design values, respectively, to avoid entrainment of the smallest drops with the feed stream. The drop diameter was therefore generally a factor of 1.4 higher than designed, which caused a 2.5 times lower specific area and a decrease in the number of equilibrium stages over the column length. The designed extraction efficiency was nevertheless achieved, since the extraction factor E was 1.6 times higher than in the original design and the safety margin in the column length was sufficient.

The auxiliary equipment in the extraction process consisted of an electrostatic splitter and an emulsifying device. The electrostatic splitter removed 85% of the strip phase from the loaded emulsion at a frequency of 3 kHz and a voltage of 4 kV. Its capacity proved to be critical when the average strip droplet sizes were below 8 μm.

The validity of using the design rules for a solvent extraction RDC for the design of an ELM process was checked by comparing calculated parameter values with experimental ones. The actual and calculated values of the characteristic velocity in the column coincided well, and the values of the mass transfer coefficients reasonably. Therefore, the concepts of solvent extraction column design can be used to advantage in ELM, provided that the drop size can be predicted.

APPENDIX: DETAILED CALCULATION OF THE COLUMN DIMENSIONS (TABLE 9)

Determination of Hold-Up and Velocities

The required emulsion/feed phase ratio $\alpha_{disp,feed}$ is calculated from m_{real} and $\alpha_{str,org}$:

$$\alpha_{disp,feed} = \frac{1}{\alpha_{strip,org}} \frac{1}{m_{real}} \qquad \text{(A1)}$$

MARCEL DEKKER, INC.
270 Madison Avenue, New York, New York 10016

TABLE 9
Values of the Intermediate Parameters in the Calculation as Described in the Text

Parameter	RDC column		Spray column	
	Continuous phase	Disperse phase	Continuous phase	Disperse phase
Phase ratio $\alpha_{disp,feed}$ (—)	0.16			
Hold-up at flooding $h_{flooding}$ (—)	0.21			
Characteristic velocity u_0 (m/s)	0.034			
Specific area a (m^2/m^3)	945			
Reynolds number Re (—)	33.5		33.5	
Schmidt number Sc (—)	1.39×10^3		1.39×10^3	
Mass transfer coefficients k_c, k_d (m/s)	6.8×10^{-5}	2.7×10^{-6}	6.2×10^{-5}	2.7×10^{-6}
HTU_c, HTU_d (m)	0.10	0.40	0.22	0.81
Dispersion coefficients D_{ec}, D_{ed} (—)	1.3×10^{-4}	2.3×10^{-4}	1.2×10^{-4}	2.0×10^{-4}
HDU_{oc}	0.040		0.017	
HTU_{oc}	0.22		0.27	
HTU	0.38		0.74	
HETS	0.48		0.93	
Number of stages n_{th} (—)	4.5			

With this value, the hold-up at flooding $h_{flooding}$ is determined (16):

$$\alpha_{disp,feed} = \frac{2h_{flooding}^2 - h_{flooding}^3}{(1 - h_{flooding})^3} \tag{A2}$$

The work hold-up h is 0.75 times the hold-up at flooding. Then the characteristic velocity u_0 is determined from Eq. (A3) (15). The slip velocity u_s is related to the characteristic velocity via the hold-up h. The same equation is found in Klee and Treybal (38):

$$\frac{4}{3}\frac{\Delta\rho d_{32} g}{\rho_c u^2{}_0} = \left[\frac{\eta_c}{u_0 d_{32}\rho_c}\right]^{1/5} \tag{A3}$$

$$u_s = u_0 e^{-h} \tag{A4}$$

With u_0 and h, the superficial velocities of both phases with regard to the smallest cross-sectional area can be calculated (16): $u_{c,S}$ and $u_{d,S}$.

$$u_{c,S} = \frac{u_0 e^{-h}}{\frac{\alpha_{disp,feed}}{h} + \frac{1}{1-h}} \tag{A5}$$

MARCEL DEKKER, INC.
270 Madison Avenue, New York, New York 10016

$$u_{d,S} = \alpha_{disp,feed} u_{c,S} \tag{A6}$$

The smallest column opening is calculated from $u_{c,S}$. This is the stator opening S for the RDC, and the column diameter D_{col} for the spray column, calculated from

$$\begin{aligned} \text{RDC: } \frac{\pi}{4} S^2 &= \varphi_{feed}/u_{c,S} \\ \text{Spray: } \frac{\pi}{4} D_{col}^2 &= \varphi_{feed}/u_{c,S} \end{aligned} \tag{A7}$$

For the RDC, the diameter of the column D_{col}, the rotor diameter R, and the compartment height H follow from the relations (15)

$$\begin{aligned} S &= 0.7 D_{col} \\ R &= 0.5 D_{col} \\ H &= 0.3 D_{col} \end{aligned} \tag{A8}$$

Slightly different ratios between S, R, H, and D_{col} are given in Ref. 16 (0.7, 0.6, and 1.5, respectively), whereas Ref. 14 recommends 0.67, 0.5, and $H = 0.62 D_{col}^{0.68}$.

$u_{c,Dcol}$ and $u_{d,Dcol}$, the superficial velocities based on column diameter, can be defined

$$u_{c,Dcol} = \frac{S^2}{D_{col}^2} u_{c,S}, \qquad u_{d,Dcol} = \frac{S^2}{D_{col}^2} u_{d,S} \tag{A9}$$

The critical rotor speed N_{cr} for drops to stay dispersed in the RDC is calculated using Eq. (A8) (14). The actual rotor speed N lies a factor 1.2 higher:

$$\begin{aligned} \frac{g}{R N_{cr}^2} \left[\left(\frac{\gamma^3 \rho_c}{\eta^4_c g} \right)^{0.25} \left(\frac{\Delta\rho}{\rho_c} \right)^{0.6} \right]^{0.5} &= 16 \\ N &= 1.2 N_{cr} \end{aligned} \tag{A10}$$

Calculation of the Column Height

Re and Sc are calculated to insert in the mass transfer coefficient equations:

$$\text{Re} = \frac{d_{32} \rho_c u_0}{\eta_c}, \qquad \text{Sc} = \frac{\eta_c}{\rho_c I D_c} \tag{A11}$$

The mass transfer coefficients were calculated from various empirical relations. The relationship used for k_d gave results that were of the same order as values found in a lab-scale experiment (14) and formed a conservative choice from the available equations.

$$\text{RDC and Spray:} \qquad k_d = \frac{2\pi^2 I D_d}{3 d_{32}} \tag{A12}$$

$$\text{RDC:} \qquad k_c = (50 + 0.0085 \text{ReSc}^{0.7})(ID_c/d_{32}) \tag{A13}$$

$$\text{Spray:} \qquad k_c = 0.725 u_s (1 - h)(\text{Re}e^{-h})^{-0.43}\text{Sc}^{-0.58} \tag{A14}$$

$$\frac{1}{k_{oc}} = \frac{1}{k_c} + \frac{1}{m_{f,disp} k_d} \tag{A15}$$

The superficial velocities related to the column diameter $u_{c,Dcol}$ and $u_{d,Dcol}$ must be used for the calculation of HTU_c and HTU_d:

$$\text{HTU}_c = \frac{u_{c,Dcol}}{a_{spec} k_c}, \qquad \text{HTU}_d = \frac{u_{d,Dcol}}{a_{spec} k_d}, \qquad \text{where } a_{spec} = 6h/d_{32} \tag{A16}$$

$$\text{HTU}_{oc} = \text{HTU}_c + (\text{HTU}_d/\text{E}) \tag{A17}$$

The axial dispersion coefficients D_{ec} and D_{ed} are given by

$$D_{ec} = \frac{0.5 u_{c,Dcol} H}{(1 - h)} + 0.012 RNH \left(\frac{S}{D_{col}}\right)^2 \tag{A18}$$

$$D_{ed} = \frac{u_{d,Dcol} H}{h} + 0.024 RNH \left(\frac{S}{D_{col}}\right)^2 \tag{A19}$$

With these values, HDU_{oc} for little axial dispersion (16) and HTU can be calculated, and finally the value of HETS (16):

$$\text{HDU}_{oc} = \frac{(1 - h) D_{ec}}{u_{c,Dcol}} + \frac{h D_{ed}}{u_{d,Dcol} E} \tag{A20}$$

$$\text{HTU} = \text{HTU}_{oc} + \text{HDU}_{oc} \tag{A21}$$

$$\text{HETS} = \frac{\ln(E)}{1 - \frac{1}{E}} \text{HTU} \tag{A22}$$

MARCEL DEKKER, INC.
270 Madison Avenue, New York, New York 10016

The number of equilibrium stages is calculated using (14)

$$n_{\text{th}} = \ln\left[\frac{[Cd]_{\text{feed,in}} - \frac{1}{m}[Cd]_{\text{disp,in}}}{[Cd]_{\text{feed,out}} - \frac{1}{m}[Cd]_{\text{disp,in}}}\left(1 - \frac{1}{E}\right) + \frac{1}{E}\right](\ln E)^{-1} \quad \text{(A23)}$$

To obtain H_{col}, the height of the column n_{th} is multiplied with the HETS (16):

$$H_{\text{col}} = \text{HETS} n_{\text{th}} \quad \text{(A24)}$$

This amounted to a height H_{col} of 2.2 m for the RDC column and 4.2 m for the spray column. For the spray column, the method proposed by Laddha and Degaleesan (14) was also used. It produced a required column height of 3.2 m.

Splitter Design

The radius of the splitter is found from φ_{disp}, τ_{splitter}, and the L/r_{splitter} ratio. The diameter of the center electrode is chosen. The capacitance C for round capacitors can be calculated as follows:

$$C = \frac{2\pi\varepsilon_0\varepsilon_r L}{\ln(r_{\text{splitter}}/r_i)} \quad \text{(A25)}$$

The impedance Z is dependent on the design frequency f and is given by

$$Z = \frac{1}{2\pi f C} \quad \text{(A26)}$$

Then the current I can be calculated from V and Z according to Ohms law, and the power requirement follows.

Additional Equations for Calculation of u_0

Barnea–Mizrahi (BM) (39): The slip velocity $u_{s,i}$ of a drop i must be solved using Re_i

$$\frac{4d_i g\Delta\rho(1-h)}{3u_{s,i}^2\rho_c(1+h^{1/3})} = \left(0.63 + \frac{4.8}{\text{Re}_i^{1/2}}\right)^2, \qquad \text{where} \qquad \text{Re}_i = \frac{d_i u_{s,i}\rho_c}{\eta_c} \quad \text{(A27)}$$

Barnea–Mizrahi–Korchinsky (39): The BM slip velocity is corrected with a constriction factor C_R:

MARCEL DEKKER, INC.
270 Madison Avenue, New York, New York 10016

$$C_R = \frac{\dfrac{u_d}{h} + \dfrac{u_c}{(1-h)}}{\sum_i f_i u_{s,i}}, \qquad \text{with} \qquad u_{s,i\text{BMK}} = C_R u_{s,i\text{BM}} \tag{A28}$$

Kumar and Hartland (40): With $k_1 = -3.25 \times 10^{-2}$ and $k_2 = 0.3$ for transport to the disperse phase:

$$\frac{u_{s,i}\rho_c^{1/4}}{g^{1/4}\gamma^{1/4}} = (k_1 + k_2 e^{-1.28N^2R/g}) \left(\frac{\Delta\rho}{\rho_c}\right)^{0.52} \left(\frac{\eta_c g^{1/4}}{\rho_c^{1/4}\gamma^{3/4}}\right)^{-0.45} \left(\frac{R^2\rho_c g}{\gamma}\right)^{0.08} \left(\frac{H}{R}\right)^{1.03} \left(\frac{R}{D_{col}}\right)^{0.51} \left(\frac{u_d\rho_c^{1/4}}{g^{1/4}\gamma^{1/4}}\right)^{0.28} \tag{A29}$$

SYMBOLS

a_{spec}	specific interfacial area feed/disperse phase (m^2/m^3)
C	concentrations ($kmol/m^3$); capacitance splitter (F)
C_R	constriction factor (in calculation u_0 according to Korchinsky)
d; d_{32}	drop diameter; Sauter mean diameter (m)
D_{col}	column diameter (m)
D_{ec}	axial dispersion coefficient continuous (feed) phase (m^2/s)
D_{ed}	axial dispersion coefficient disperse phase (m^2/s)
ID_c	diffusion coefficient continuous (feed) phase (m^2/s)
ID_d	diffusion coefficient disperse phase (m^2/s)
E	extraction factor (—)
f	frequency of AC current in splitter (Hz)
f_i	frequency of size class i (—)
g	gravity acceleration (m/s^2)
H	compartment height (m)
H_{col}	column height (m)
h	hold-up (—)
$h_{flooding}$	hold-up at flooding (—)
HETS	height equivalent of a theoretical stage (m)
HDU_{oc}	height of a diffusion unit, overall continuous phase (m)
HTU	height of a transfer unit, including axial dispersion, overall (m)
HTU_c, HTU_d	height of a transfer unit, continuous (feed) and disperse phase, respectively (m)

HTU_{oc}	height of a transfer unit, overall continuous (feed) phase (m)
I	current through splitter (A)
k_c; k_d	mass transfer coefficient continuous (feed) and disperse phase, respectively (m/s)
k_{oc}	overall mass transfer coefficient (m/s) based on continuous phase
L	splitter length (m)
m_{real}	actual concentration factor (—)
m_{feed}; m_{strip}	equilibrium distribution coefficients organic/feed c.q. strip/organic (—)
m_{feeds}; $m_{feed,disp}$	deducted distribution coefficients strip/feed c.q. disperse/feed (—)
N	rotor speed (s^{-1})
N_{cr}	critical rotor speed above which drops stay dispersed in the column (s^{-1})
$n_{calc,HETS}$; n_{meas}	number of stages, calculated with measured HETS; measured (—)
n_{th}	number of theoretical stages (—)
R	rotor diameter (m)
$r_{splitter}$; r_i	splitter radius; splitter internal electrode radius (m)
Re	Reynolds number (—)
S	diameter stator opening (m)
Sc	Schmidt number (—)
$u_{c,S}$; $u_{c,Dcol}$	superficial velocity continuous (feed) phase relative to stator diameter S and column diameter D_{col}, respectively (m/s)
$u_{d,S}$; $u_{d,Dcol}$	superficial velocity disperse phase relative to stator diameter S and column diameter D_{col}, respectively (m/s)
u_0	characteristic velocity (m/s)
u_s	slip velocity (m/s)
V	applied voltage splitter (V)
Z	impedance splitter (Ω)

Greek

$\alpha_{disp,feed}$	volume ratio disperse (emulsion):feed phase
$\alpha_{strip,org}$	volume ratio strip:organic phase in emulsion
γ	interfacial tension disperse/feed phase (N/m)
ε_0	permittivity of vacuum (8.854×10^{-12} $C^2 \cdot J^{-1} \cdot m^{-1}$)

MARCEL DEKKER, INC.
270 Madison Avenue, New York, New York 10016

ε_r	relative dielectric constant (—)
η_c, η_d	viscosity continuous; disperse phase (Pa·s)
ρ_c; ρ_d	density continuous (feed); disperse phase (kg/m^3)
$\Delta\rho$	density difference continuous and disperse phase (kg/m^3)
τ_{column}; $\tau_{splitter}$	residence time of disperse phase in column; c.q. in splitter (s)
φ_{feed}; φ_{disp}	flow rate feed; disperse (m^3/s)

Subscripts

BM	according to Barnea–Mizrahi
BMK	according to Korchinsky
d, disp	disperse phase
f, feed, c	feed (continuous) phase
i	for the individual droplet *i*
org	organic (membrane) phase
s, strip	strip phase

ACKNOWLEDGMENTS

H. H. Poortinga and R. A. P. Zwinkels are kindly acknowledged for their contribution to this work.

REFERENCES

1. J. Draxler and R. Marr, *Chem. Eng. Process., 20*, 319–329 (1986).
2. H. C. Hayworth, W. S. Ho, W. A. Burns, and N. N. Li, *Sep. Sci. Technol., 18*, 493–521 (1983).
3. P. Becker, *Phosphates and Phosphoric Acid*, 2nd ed., Dekker, New York, NY, 1989.
4. H. Reisinger, "Aufarbeitung von Bioprodukten durch Flussig-Membran-Permeation," Thesis, Technische Universität Graz, 1992, p. 44.
5. J. Draxler, *Flüssige Membranen für die Abwasserreinigung*, Institut für Thermische Verfahrenstechnik und Umwelttechnik, Technische Universität Graz, 1992.
6. F. Nakashio, M. Goto, M. Matsumoto, J. Irie, and K. Kondo, "Role of Surfactants in the Behaviour of Emulsion Liquid Membranes—Development of New Surfactants," *J. Membr. Sci., 38*, 249–260 (1988).
7. P. R. Danesi, R. Chiarizia, and A. Castagnola, "Transfer Rate and Separation of Cd(II) and Zn(II) Chloride Species by a Trilaurylammonium Chloride–Triethylbenzene Supported Liquid Membrane, *Ibid., 14*, 161–174 (1983).
8. Y. C. Hoh, C. Y. Lin, T. M. Hung, and T. M. Chiu, "Separation of Cadmium from Zinc in a Chloride Media by a Supported Liquid Membrane," in *Proc. ISEC 1990* (T. Sekine, Ed.), 1990, pp. 1543–1548.

9. G. R. M. Breembroek, "Emulsion and Supported Liquid Membrane Extraction of Copper and Cadmium," Thesis, Delft UT, 1998, Chap. 3 (ISBN 90-802879-7-0).
10. M. Muhammed, M. Valiente, M. Aguilar, and M. Masana, "Separation of Base Divalent Metals from Chloride Solutions by Solvent Extraction Processes," *Chem. Scr., 29*, 149–153 (1989).
11. T. A. Hatton and D. S. Wardius, "Analysis of Staged Liquid Surfactant Membrane Operations," *AIChE J., 30*, 934–944 (1984).
12. P. Walstra, in *Encyclopedia of Emulsion Technology, Vol. 1: Basic Theory* (P. Becher, Ed.), Dekker, New York, NY, 1983, pp. 64–127.
13. E. C. Hsu and N. N. Li, "Membrane Recovery in Liquid Membrane Separation Processes," *Sep. Sci. Technol., 20*(2&3), 115–130 (1985).
14. G. S. Laddha and T. E. Degaleesan, *Transport Phenomena in Liquid Extraction*, Tata McGraw-Hill, New Delhi, 1976.
15. F. J. Zuiderweg, *Fysische Scheidingsmethoden, Deel 2*, Technical University Delft, 1987.
16. T. C. Lo, M. H. I. Baird, and H. Hanson (Eds.), *Handbook of Solvent Extraction*, Wiley, New York, NY, 1983.
17. K. K. Al-Aswad, C. J. Mumford, and G. V. Jeffreys, "The Application of Drop Size Distribution and Discrete Drop Mass Transfer Models to Assess the Performance of a Rotating Disc Contactor," *AIChE J., 31*, 1488–1497 (1985).
18. A. M. Hochhauser and E. L. Cussler, "Concentrating Chromium with Liquid Surfactant Membranes," *AIChE Symp. Ser., 152*(71), 136–142 (1975).
19. W. S. Ho, T. A. Hatton, E. N. Lightfoot, and N. N. Li, "Batch Extraction with Liquid Surfactant Membranes: A Diffusion Controlled Model," *AIChE J., 28*, 662–670 (1982).
20. A. L. Bunge and R. D. Noble, "A Diffusion Model for Reversible Consumption in Emulsion Liquid Membranes," *J. Membr. Sci., 21*, 55–71 (1984).
21. C. C. Lin and R. L. Long, "Phenol Removal by Emulsion Liquid Membrane: A Modified Diffusion Model," *Chem. Eng. Commun., 156*, 45–58 (1996).
22. C. C. Lin and R. L. Long, "Removal of Nitric by Emulsion Liquid Membrane: Experimental Results and Model Prediction," *J. Membr. Sci., 14*, 33–45 (1997).
23. C. C. Wang and A. L. Bunge, "Multisolute Extraction of Organic Acids by Emulsion Liquid Membrane. II. Continuous Experiments and Model," *Ibid., 53*, 105–126 (1990).
24. C. C. Chan and C. J. Lee, "Mechanistic Models of Mass Transfer across a Liquid Membrane," *Ibid., 20*, 1–24 (1984).
25. R. Rautenbach and O. Machhammer, "Modeling of Liquid Membrane Separation Processes," *Ibid., 36*, 425–444 (1988).
26. D. M. Lorbach and T. A. Hatton, "Polydispersity and Backmixing Effects in Diffusion Controlled Mass Transfer with Irreversible Chemical Reaction: An Analysis of Liquid Emulsion Membrane Processes," *Chem. Eng. Sci., 43*(3), 405–418 (1988).
27. H. J. Bart, A. Bauer, L. D. Lorbach, and R. Marr, "Auslegungskriterien fuer die Extraktion met chemischer Reaktion und Fluessigmembran-Permeation," *Chem.-Ing.-Tech., 60*, 169–179 (1988).
28. R. Marr and A. Kopp, "Liquid Membrane Technology—A Survey of Phenomena, Mechanisms, and Models," *Int. Chem. Eng., 22*(1), 44–60 (1982).
29. C. R. Wilke and P. Chang, "Correlation of Diffusion Coefficients in Dilute Solutions," *AIChE J., 1*, 264–270 (1955).
30. P. J. Bailes and S. K. L. Lakai, "An Experimental Investigation into the Use of High Voltage d.c. Fields for Liquid Phase Separation, *Trans. Inst. Chem. Eng., 59*, 229–237 (1981).
31. A. Kriechbaumer and R. Marr, "Emulsion Breaking in Electric Fields," *ACS Symp. Ser., 272*, 381–398 (1985).
32. M. Goto, J. Irie, K. Kondo, and F. Nakashio, "Electric Demulsification of w/o Emulsion by Continuous Tubular Coalescer," *J. Chem. Eng. Jpn., 22*(4), 401–406 (1989).

MARCEL DEKKER, INC.
270 Madison Avenue, New York, New York 10016

33. C. Tsouris, V. I. Kirou, and L. L. Tavlarides, "Drop Size Distribution and Hold-up Profiles in a Multistage Extraction Column," *AIChE J., 40*, 407–418 (1994).
34. V. I. Kirou, L. L. Tavlarides, J. C. Bonnet, and C. Tsouris, "Flooding, Hold-up, and Drop Size Measurements in a Multistage Column Extractor," *Ibid., 34*(2), 283–292 (1988).
35. C. J. Mumford and A. A. A. Al Hemiri, "The Effect of Wetting Characteristic upon the Performance of a Rotating Disc Contactor," *ISEC '74, 2*, 1591–1619 (1974).
36. S. Sarkar, C. R. Phillips, and C. J. Mumford, "Characterization of Hydrodynamic Parameters in Rotating Disc and Oldshue-Rushton Columns. Hydrodynamic Modelling, Drop Size, Hold-up and Flooding," *Can. J. Chem. Eng., 63*, 701–709 (1985).
37. Reference 9, Chap. 6.
38. A. J. Klee and R. E. Treybal, "Rate of Rise and Fall of Liquid Drops," *AIChE J., 2*, 444–447 (1956).
39. W. J. Korchinsky and R. Al-Husseini, "Liquid-Liquid Extraction Column (Rotating Disc Contactor)-Model Parameters from Drop-Size Distribution and Solute Concentration Measurements," *J. Chem. Tech. Biotechnol., 36*, 395–409 (1986).
40. A. Kumar and S. Hartland, "Independent Prediction of Slip Velocity and Hold-up in Liquid-Liquid Extraction Columns," *Can. J. Chem. Eng., 67*, 17–25 (1989).

Received by editor January 29, 1999
Revision received December 1999

Request Permission or Order Reprints Instantly!